New Insights into Structure and Luminescence of Eu^III and Sm^III Complexes of the 3,4,3-LI(1,2-HOPO) Ligand

Lena J. Daumann,[†] David S. Tatum,[†] Benjamin E. R. Snyder,[‡] Chengbao Ni,[†] Ga-lai Law,[†] Edward I. Solomon,[‡] and Kenneth N. Raymond*,[†]

[†]Chemical Science Division, Lawrence Berkeley National Laboratory, and Department of Chemistry, University of California, Berkeley, California 94720, United States

[‡]Department of Chemistry, Stanford University, Stanford, California 94305, United States

S Supporting Information

ABSTRACT: We report the preparation and new insight into photophysical properties of luminescent hydroxypyridonate complexes $[M^{III}L]^-$ (M = Eu or Sm) of the versatile 3,4,3-LI(1,2-HOPO) ligand (**L**). We report the crystal structure of this ligand with Eu^III as well as insights into the coordination behavior and geometry in solution by using magnetic circular dichroism. In addition TD-DFT calculations were used to examine the excited states of the two different chromophores present in the 3,4,3-LI(1,2-HOPO) ligand. We find that the Eu^III and Sm^III complexes of this ligand undergo a transformation after in situ preparation to yield complexes with higher quantum yield (QY) over time. It is proposed that the lower QY in the in situ complexes is not only due to water quenching but could also be due to a lower degree of f-orbital overlap (in a kinetic isomer) as indicated by magnetic circular dichroism measurements.

L igand-sensitized luminescent lanthanide(III) complexes have unique photophysical properties, which make them exciting candidates for a wide range of applications, including fluorescence-based bioassays; as has been extensively reviewed.[1−5] We have shown that the 6-amide derivatives of 1-hydroxy-pyridin-2-one (1,2-HOPO) in tetradentate ligands form Eu^III complexes with high thermodynamic stability ($pEu^{7.4} \approx 18.6$) and excellent photophysical properties (quantum yields up to 21.5%).[6] This chromophore has also been previously shown to efficiently sensitize Sm^III. Studies of the aryl bridged tetradentate 1,2-HOPO ligands have shown that the geometries of the ligand backbones significantly affect the quantum yields of the corresponding europium complexes.[7] We have also recently confirmed the sensitization and emission efficiencies of those 1,2-HOPO complexes by time-resolved X-ray absorption near edge structure measurements at the Eu L3 edge.[8] Octadentate ligands, such as the branched H(2,2)-1,2-HOPO ligand and the linear spermine linked 3,4,3-LI(1,2-HOPO) ligand (**LH₄**, Scheme 1) form significantly more stable europium complexes ($pEu^{7.4} > 21.2$) than tetradentate 1,2-HOPO ligands.[9,10] The 3,4,3-LI(1,2-HOPO) ligand (**LH₄**) has been reported as an efficient actinide sequestration agent *in vivo*, however, the detailed coordination behavior toward Ln(III) and An(III) ions of this ligand are to date unknown.[10−16] This ligand has also been discussed as a

Scheme 1. Spermine-Linked 3,4,3-LI(1,2-HOPO) Ligand for Sensitization of Eu^III and Sm^III (Coordinating Atoms in Red)
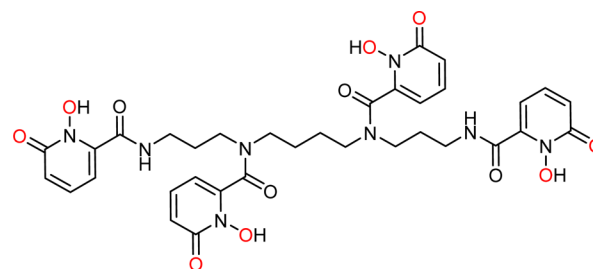
chelator for ⁸⁹Zr radiopharmaceuticals.[17] Abergel et al. recently demonstrated the capability of **L** to act as an effective chelator for Cm^III while also sensitizing Cm^III photoluminescence, with a long lifetime (383 μs) and a remarkable quantum yield in water (45%).[18] Previously, the Eu^III and Sm^III complexes have been prepared *in situ* and QYs of 7.0 and 0.2% have been reported.[9] We propose that upon mixing **L** with Eu^III (and Sm^III) two isomers form, A and B. A is a kinetic product that slowly converts fully to the brighter thermodynamic isomer, B.

The isolated complexes $[ML][C_5H_6N]$ were prepared by refluxing a 1:1 mixture of **LH₄** and the corresponding M^III salt in methanol using pyridine as base, yielding the complexes as white solids. Experimental details and mass spectral data can be found in the Supporting Information (Figures S1−S3). X-ray-quality crystals of $[EuL]K(DMF)$ were obtained by slow diffusion of a mixture of THF and cyclohexane into a DMF solution containing the complex and KCl. As shown in Figure 1, a ML complex is formed, in which the Eu^III ion is coordinated to eight oxygen atoms from the four 1,2-HOPO units. In addition, a K⁺ ion and a highly ordered DMF molecule are present in the crystal lattice, which show intermolecular interactions with the $[EuL]^-$ units to form a one-dimensional chain (Figures S4 and S5). The Eu−O distances in $[EuL]^-$ range from 2.36 to 2.44 Å and are similar to previously reported tetradentate 1,2-HOPO complexes.[6] Crystallographic parameters and selected bond lengths can be found in Tables S1 and S2. There are two types of 1,2-HOPO units present within the ligand and Ln^III complexes. Two of the 1,2-HOPO units are connected to the backbone by secondary amide groups (N5
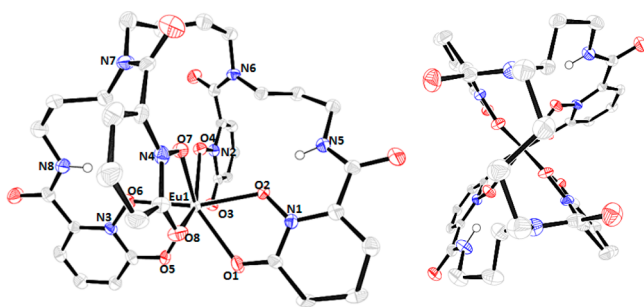
Figure 1. X-ray structure of $[EuL]^-$ (50% probability) without hydrogen atoms, except for the amide hydrogens (NH). Left, side on view; right, top view through C_2 axis.

and N8), which show intramolecular hydrogen bonding interactions ($N-H\cdots O \approx 1.85$ Å) with the adjacent $O_{N\text{-oxide}}$ atoms (O2 and O6). In accordance, the secondary amides show coplanarity with their 1,2-HOPO units (torsion angles ≈ 3.0 and 8.7°), ensuring that the π systems of the amide functions maintain conjugation with the corresponding 1,2-HOPO units. The tertiary amide groups, however, display large torsion angles (ca. 62.1 and 64.0°) relative to the respective 1,2-HOPO planes, which partially breaks the aforementioned π-conjugation. Such dramatic differences highlight the importance of intramolecular $N-H\cdots O$ hydrogen bonding interactions for preorganization of the ligand. Gas-phase DFT ground state minimization (B3LYP//6-31G(d,p)) of $[EuL]^-$ closely matches the crystal structure. Only one of the four 1,2-HOPO units deviates significantly from its superposed partner, which is likely due to crystal packing effects in the solid state, including interactions with the K^+ ion and solvent (Figure S6). The shape measurements[19] of the calculated and crystal structure yield slightly different results. While the crystal structure shows a slight preference for a C_{2v} symmetry the calculated structure yields a dodecahedral (D_{2d}) geometry for the coordinating oxygen atoms around the Eu^{III} ion (Table S3).

For the isolated Eu^{III} and Sm^{III} complexes, quantum yields of 15.6% and 0.41% were measured in aqueous solution ($\lambda_{ex} = 325$ nm). In addition, a new protocol reported here for the *in situ* preparation (the samples were prepared by combining L and M^{III} in TRIS buffer and measuring photophysical data no later than 10 minutes after mixing) yields similar yet slightly lower QYs for $[EuL]^-$ and $[SmL]^-$ (14.0% and 0.39%, respectively). Notably the initially measured (T=0) luminescence QYs of the *in situ* Eu^{III} and Sm^{III} complexes increased over time (2–4 h, Figure 2) to reach the values of the isolated complexes (Figures S9–S11). We do not attribute this effect to slow complexation, since no luminescence from free ligand was observed. We conclude that the lower QY for the *in situ* generated complex is
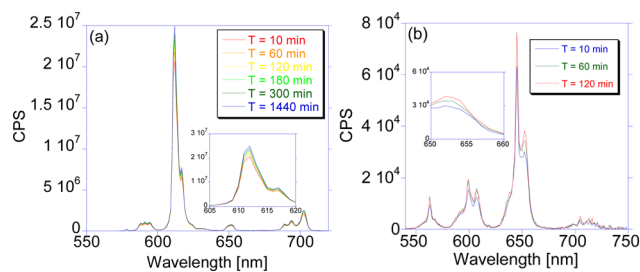
due to slow rearrangement of some fraction (a kinetic isomer) of the initially formed complex.

First-order luminescence decay measurements indicated that the number of bound water molecules in $[EuL]^-_{isolated}$ is essentially zero ($q = 0.04$).[20] We have also considered the possibility of dimeric Eu_2L_2 complex formation. However, upon serial dilution of the complexes ($2 \times 10^{-5} - 5 \times 10^{-6}$ M) the luminescence lifetimes measured remained unchanged. The lifetimes were best fit to a mono exponential decay, consistent with but not conclusive of one species in solution. Intriguingly the measured lifetimes (τ_{obs}) in H_2O and D_2O for $[EuL]^-_{isolated}$ were longer than for $[EuL]^-_{in\ situ}$ (Table 1). A slightly increased q

Table 1. Photophysical Parameters for $[EuL]^-$ ($\lambda_{ex} = 325$ nm)

	isolated	*in situ* ($T = 0$)
k_{rad} [s^{-1}]	586 ± 60	587 ± 63
τ_{rad} [μs]	1705 ± 177	1721 ± 180
η_{Eu}	0.469 ± 0.016	0.417 ± 0.045
η_{sens}	0.397 ± 0.018	0.356 ± 0.043
QY [%]	15.6 ± 0.6	14.0 ± 0.3
q	0.04	0.14
τ_{H_2O} [μs]	814 ± 8	711 ± 7
τ_{D_2O} [μs]	1135 ± 9	1030 ± 6
k_{nonrad} [s^{-1}]	623 ± 60	792 ± 62

value for the *in situ* complex could indicate that a portion of the formed complex (isomer A) leaves the Eu^{III} sites open for coordination of a water molecule. A similar observation was found for $[SmL]^-$ where lifetimes in H_2O and D_2O for the isolated complex were longer (19.4 ± 0.1 and $180.9 \pm 0.6\ \mu s$) than for the in situ complex (18.4 ± 0.1 and $155.0 \pm 0.3\ \mu s$), respectively. The conversion of kinetic isomer A to the longer lived B is also provided by an experiment which showed that τ_{obs} of *in situ* generated complex converged toward the τ_{obs} of the isolated complex (Figure S12).

A close examination of the photophysical parameters was conducted. For the Eu^{III} complex, the parameters in Table 1 can be obtained from the ratio of the magnetic dipole transition ($^5D_0 \rightarrow {}^7F_1$) intensity to the total emission intensity, from which the radiative lifetime (τ_{rad}) can be estimated.[7,21,22] Analysis showed that the metal and sensitization efficiencies η_{Eu} and η_{sens} are similar within error for both methods of preparation (Table 1). The most significant difference is seen for k_{nonrad} which is higher (792 s^{-1}) for the *in situ* complex, thus the lower QY is attributed to increased rates of nonradiative quenching. The q value is higher (0.14) for the *in situ* complex but over time (~2 h) reaches the value of the isolated complex (0.04), suggesting that some portion of the initially formed $[EuL]^-$ rearranges, and in the process displaces the quenching water molecule.

Upon comparison of the excitation and absorption spectra of $[EuL]^-$ and with the aid of TD-DFT calculations we also found that the chromophore absorbing at longer wavelength (*NH*-1,2-HOPO) is better at sensitizing Eu^{III} than the one at shorter wavelength (*N*-1,2-HOPO, Figures S7, S8, and S13, Table S4). Consistent with the differences between the excitation and absorption spectrum, we observed that the quantum yield increases upon red-shifting the excitation wavelength.

An examination of the $^5D_0 \rightarrow {}^7F_1$ transition of isolated and *in situ* $[EuL]^-$ in TRIS buffer suggests, due to the splitting into three symmetrical peaks, a low symmetry in solution (Figure S14).[23] To further analyze potential geometric differences that

Figure 2. Increase of luminescence intensity of *in situ* generated $[EuL]^-$ (a) and $[SmL]^-$ (b) measured in TRIS (pH 7.4).

might arise from the different preparation methods, we studied the magnetic circular dichroism spectra. A buffer/glycerol solvent system was unsuitable due to the poor solubility of $[ML]^-$ at high concentration, thus a 2:1 mixture of DMF and MeOH was used. The luminescence spectra of $[EuL]^-$ and $[SmL]^-$ were also recorded under these conditions and the absence of splitting of the $^5D_0 \rightarrow ^7F_1$ transition points to a higher symmetry than in buffer (Figure S15). Indeed, for both $[EuL]^-_{isolated}$ and $[EuL]^-_{in\ situ}$ a negative A-term around 465 nm, arising from the $^5D_2 \leftarrow ^7F_0$ transition, typical for D_{2d} symmetry, was found (Figure 3, Figure S16).[24] Remarkably, this is in

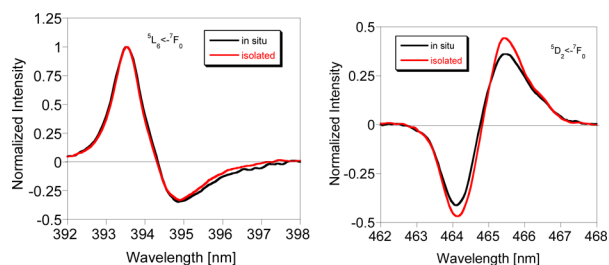**Figure 3.** Observed MCD transitions for $[EuL]^-_{isolated}$ and $[EuL]^-_{in\ situ}$ measured in DMF:MeOH (2:1) at 7 T and 250 K.

accordance with the findings from shape analysis for the DFT calculated structure. In addition we also observed the $^5L_6 \leftarrow ^7F_0$ transition.[24,25] While both methods of preparation yield similar MCD spectra, the relative intensities (based on the normalized $^5L_6 \leftarrow ^7F_0$ transition) are different (for the *in situ* prepared complex the $^5D_2 \leftarrow ^7F_0$ MCD transition is ~16% less intense). For octahedral Eu^{III} complexes the intensity ratio between the two $^5D_2 \leftarrow ^7F_0$ and $^5L_6 \leftarrow ^7F_0$ transitions has been used to describe the degree of f-orbital overlap.[26,27] If this concept is transferred to the MCD of $[EuL]^-$ it could suggest a higher degree of orbital overlap for $[EuL]^-_{isolated}$.

Combining the results from magnetic circular dichroism and the luminescence quantum yield and lifetime measurements it appears that for maximal quantum yields and optimal water shielding, complex preparation plays a crucial role. In order for L^{4-} to fully coordinate the metal ion with all four HOPO units the complexes should be isolated prior to luminescence measurements. We propose that the lower QY in the *in situ* complex is not only due to water quenching but could also be due to a lower degree of f-orbital overlap (in the kinetic isomer) as indicated by magnetic circular dichroism measurements. We are currently investigating if this technique, combined with luminescence measurements, could be potentially used to probe a Dexter mechanism of energy transfer.[28]

■ ASSOCIATED CONTENT

Ⓢ Supporting Information

Experimental procedures, crystal structure parameters, DFT calculation details, and mass spectral and photophysical data. This material is available free of charge via the Internet at http://pubs.acs.org.

■ AUTHOR INFORMATION

Corresponding Author

*raymond@socrates.berkeley.edu

Notes

The authors declare the following competing financial interest(s): This technology is licensed to Lumiphore, Inc., in which K.N.R. has a financial interest.

■ REFERENCES

(1) Zwier, J. M.; Bazin, H.; Lamarque, L.; Mathis, G. *Inorg. Chem.* **2014**, *53*, 1854.

(2) Bünzli, J.-C. G.; Eliseeva, S. V. *Chem. Sci.* **2013**, *4*, 1939.

(3) Butler, S. J.; Parker, D. *Chem. Soc. Rev.* **2013**, *42*, 1652.

(4) Faulkner, S.; Pope, S. J. A.; Burton-Pye, B. P. *Appl. Spectrosc. Rev.* **2005**, *40*, 1.

(5) Wang, X.; Chang, H.; Xie, J.; Zhao, B.; Liu, B.; Xu, S.; Pei, W.; Ren, N.; Huang, L.; Huang, W. *Coord. Chem. Rev.* **2014**, *273–274*, 201.

(6) Moore, E. G.; Xu, J.; Jocher, C. J.; Werner, E. J.; Raymond, K. N. *J. Am. Chem. Soc.* **2006**, *128*, 10648.

(7) D'Aleo, A.; Moore, E. G.; Szigethy, G.; Xu, J.; Raymond, K. N. *Inorg. Chem.* **2009**, *48*, 9316.

(8) Pacold, J. I.; Tatum, D. S.; Seidler, G. T.; Raymond, K. N.; Zhang, X.; Stickrath, A. B.; Mortensen, D. R. *J. Am. Chem. Soc.* **2014**, *136*, 4186.

(9) Abergel, R. J.; D'Aléo, A.; Ng Pak Leung, C.; Shuh, D. K.; Raymond, K. N. *Inorg. Chem.* **2009**, *48*, 10868.

(10) Sturzbecher-Hoehne, M.; Clara, N. P. L.; D'Aleo, A.; Kullgren, B.; Prigent, A. L.; Shuh, D. K.; Raymond, K. N.; Abergel, R. J. *Dalton Trans.* **2011**, *40*, 8340.

(11) Abergel, R. J.; Durbin, P. W.; Kullgren, B.; Ebbe, S. N.; Xu, J.; Chang, P. Y.; Bunin, D. I.; Blakely, E. A.; Bjornstad, K. A.; Rosen, C. J.; Shuh, D. K.; Raymond, K. N. *Health Phys.* **2010**, *99*, 401.

(12) Sturzbecher-Hoehne, M.; Deblonde, G. J. P.; Abergel, R. J. *Radiochim. Acta* **2013**, *101*, 359.

(13) Deblonde, G. J. P.; Sturzbecher-Hoehne, M.; Abergel, R. J. *Inorg. Chem.* **2013**, *52*, 8805.

(14) Kullgren, B.; Jarvis, E. E.; An, D. D.; Abergel, R. J. *Toxicol. Mech. Methods* **2013**, *23*, 18.

(15) An, D. D.; Villalobos, J. A.; Morales-Rivera, J. A.; Rosen, C. J.; Bjornstad, K. A.; Gauny, S. S.; Choi, T. A.; Sturzbecher-Hoehne, M.; Abergel, R. J. *Int. J. Radiat. Biol.* **2014**, *90*, 1055.

(16) Liu, M.; Wang, J.; Wu, X.; Wang, E.; Abergel, R. J.; Shuh, D. K.; Raymond, K. N.; Liu, P. *J. Pharm. Biomed. Anal.* **2015**, *102*, 443.

(17) Deri, M. A.; Ponnala, S.; Zeglis, B. M.; Pohl, G.; Dannenberg, J. J.; Lewis, J. S.; Francesconi, L. C. *J. Med. Chem.* **2014**, *57*, 4849.

(18) Sturzbecher-Hoehne, M.; Kullgren, B.; Jarvis, E. E.; An, D. D.; Abergel, R. J. *Chem.—Eur. J.* **2014**, *20*, 9962.

(19) Xu, J. D.; Radkov, E.; Ziegler, M.; Raymond, K. N. *Inorg. Chem.* **2000**, *39*, 4156.

(20) Horrocks, W. D.; Sudnick, D. R. *J. Am. Chem. Soc.* **1979**, *101*, 334.

(21) Beeby, A.; Bushby, L. M.; Maffeo, D.; Gareth Williams, J. A. *J. Chem. Soc., Dalton Trans.* **2002**, 48.

(22) Werts, M. H. V.; Jukes, R. T. F.; Verhoeven, J. W. *Phys. Chem. Chem. Phys.* **2002**, *4*, 1542.

(23) Bünzli, J. C. G.; Choppin, G. R. *Lanthanide probes in life, chemical and earth sciences: Theory and practice*; Elsevier: Amsterdam, 1989.

(24) Görller-Walrand, C.; Fluyt, L. In *Handbook on the Physics and Chemistry of Rare Earths*; Gschneidner, K. A., Vitalij, K. P., Eds.; Elsevier: Amsterdam, 2010; p 40.

(25) Binnemans, K.; Görller-Walrand, C.; Lucas, J.; Duhamel, N.; Adam, J.-L. Proceedings of the 3rd International Conference on Rare Earth Development and Applications, 1995; p 198.

(26) Görller-Walrand, C.; De Moitié-Neyt, N.; Beyens, Y.; Bünzli, J. C. *J. Chem. Phys.* **1982**, *77*, 2261.

(27) Barbanel, Y. A.; Mikhailo, N. Zh. *Neorg. Khim.* **1973**, *18*, 699.

(28) Dexter, D. L. *J. Chem. Phys.* **1953**, *21*, 836.